

Supporting Information

A multifunctional material with distinct mechanochromic and piezochromic properties: π - stacking in play

*Zeyang Ding^{ab}, Tong Lu^b, Changjiang Bi^b, Bao Li^b, Shi-Tong Zhang^b, Weiqing Xu^b
and Shimei Jiang^{*ab}*

^aEngineering Research Center of Organic/Polymer Optoelectronic Materials, Ministry of Education, College of Chemistry, Jilin University, 2699 Qianjin Street, Changchun 130012, P. R. China.

^bState Key Laboratory of Supramolecular Structure and Materials, College of Chemistry, Jilin University, 2699 Qianjin Street, Changchun 130012, P. R. China.

E-mail: smjiang@jlu.edu.cn

Materials and methods

N-(4-(1-cyano-2-phenylvinyl)phenyl)benzamide (compound 1) was synthesized according to our previous work and its ^1H , ^{13}C NMR were listed in Figure S1, S2. ^1H and ^{13}C NMR spectra were performed on a Bruker AVANCE 400 MHz spectrometer (TMS as the internal standard). Fluorescence spectra of solid were carried out using a Maya2000 Pro CCD spectrometer. Excitation spectra were performed with a Shimadzu RF-6000 spectrofluorophotometer. Quantum efficiency were obtained with Edinburgh fluorescence spectrometer (FLS920). The fluorescence microscopy images were obtained from an Olympus BX51 fluorescence microscope (the excitation wavelength was 330–385 nm). Differential scanning calorimetry (DSC) measurements were collected on a Netzsch DSC 204 at a 10 °C/min scanning rate under nitrogen. X-ray diffraction (XRD) patterns were recorded with a Rigaku D/MAX 2500/PC X-ray diffractometer. Fluorescence lifetimes were carried out with FLS980 Spectrometer. Mass spectra were recorded with a Bruker Autoflex speed TOF/TOF mass spectrometer. Raman spectra were collected by a confocal Raman system (LabRAM Aramis, Horiba Jobin-Yvon) and the excitation source was a 633 nm laser. Single-crystal X-ray diffraction data were collected on a Rigaku R-Axis RAPID diffractometer using the ω -scan mode with graphite monochromator Mo K α radiation. The structure determination was solved with direct methods using SHELXTL and refined with full-matrix least-squares on F^2 . Non-hydrogen atoms were refined anisotropically. The positions of hydrogen atoms were calculated and refined isotropically. High-pressure experiments were recorded using a diamond anvil cell

(DAC). The crystal was placed in the hole with a diameter of 200 μm . A small ruby chip was inserted into the hole for in situ pressure calibration according to the R1 ruby fluorescence method. Silicon oil was used as the pressure transmitting medium.

Crystal growth

1-B and 1-G were cultivated through vacuum deposition and solvent evaporation methods, and they crystallized together in most case. Specifically speaking, by controlling the sublimation temperature at 173 $^{\circ}\text{C}$, we obtained bulk crystal of green emission and microcrystals of blue emission. As far as solvent evaporation method was concerned, mixed solvents (THF (good solvent)/methanol (poor solvent)) were selected. After evaporation for three days, blue emissive plate crystal and green emissive sheet crystal precipitated together. After single-crystal X-ray diffraction analysis, green emissive crystals with different shapes share one crystal structure. The different XRD patterns of crystals with different shapes were attributed to the exposure of different crystal faces (Fig. S3).

Theoretical and Computational Method

The geometries of all the monomer and dimer structure were selected from 1-B and 1-G in corresponding unit cells. The HOMO/LUMOs and vertical excitation energies were calculated at the td-b3lyp/6-31g(d,p) level.

CCDC 2097646 and 2097647 contain the supplementary crystallographic data for this paper. These data can be obtained free of charge from The Cambridge Crystallographic Data Centre via www.ccdc.cam.ac.uk/data_request/cif.]

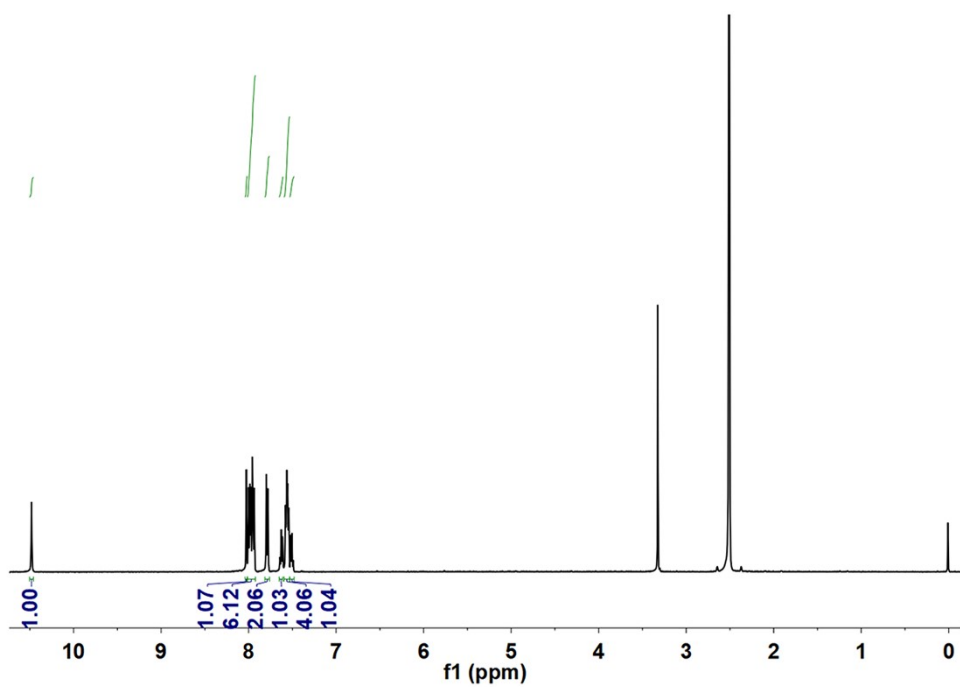


Fig. S1 ^1H NMR spectrum of compound 1 in $\text{DMSO-}d_6$.

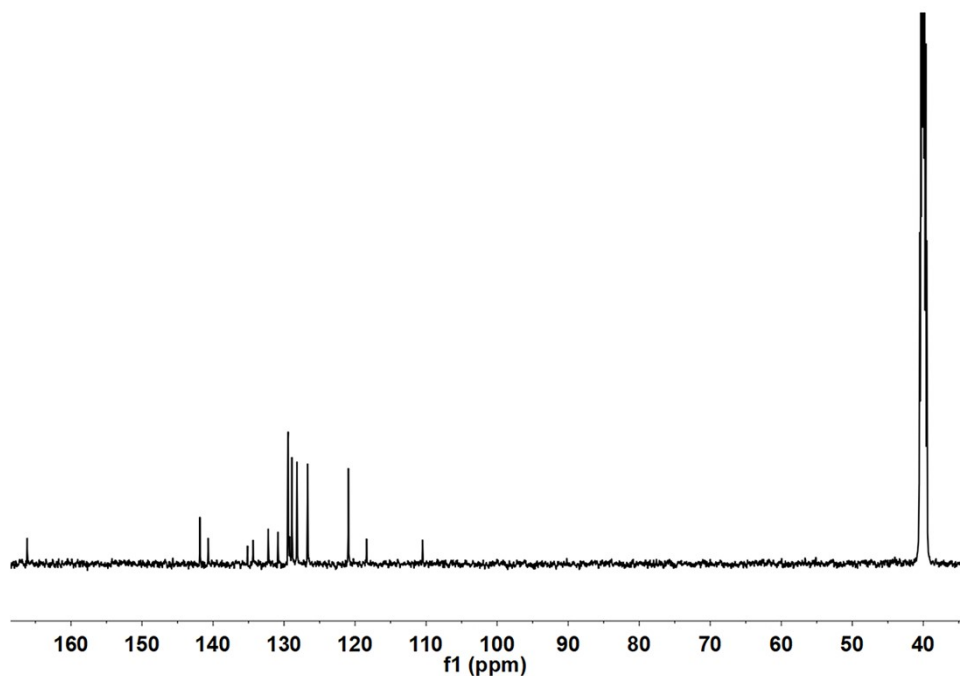


Fig. S2 ^{13}C NMR spectrum of compound 1 in $\text{DMSO-}d_6$.

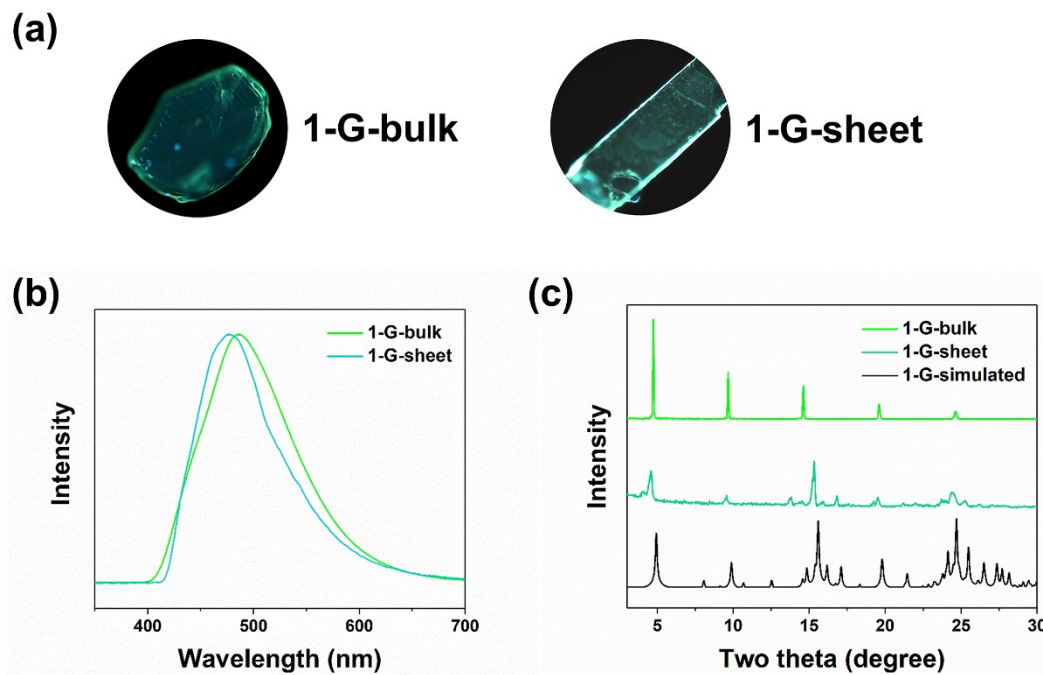


Fig. S3 (a) Fluorescence microscopic images, (b) fluorescence spectra and (c) XRD patterns of 1-G with different shapes (including its simulated XRD result). The results indicated the same crystal structure of 1-G-bulk and 1-G-sheet.

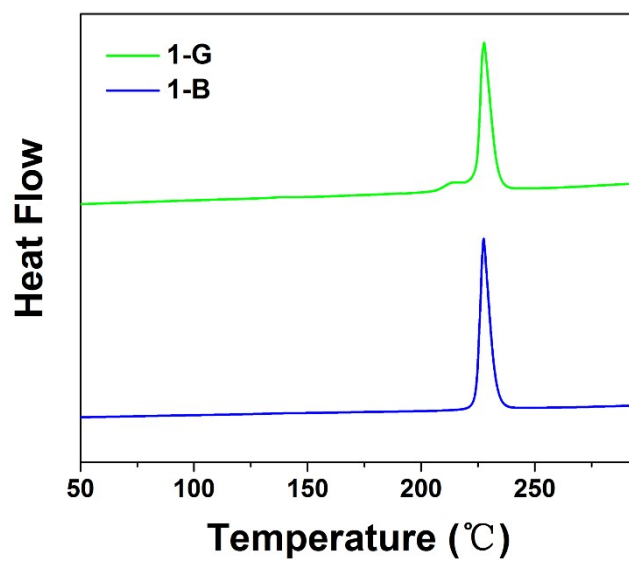


Fig. S4 DSC curves of 1-G and 1-B.

Table S1. Emission maxima, fluorescence quantum yields, lifetimes and kinetic constants of 1-B and 1-G.

	λ_{em} (nm)	τ_{av} (ns)	τ (ns)	ϕ_F	k_r (ns ⁻¹)	k_{nr} (ns ⁻¹)
1-B	440	2.51	1.23 (0.13), 2.60 (0.87)	31%	0.124	0.275
1-G	486	4.33	2.39 (0.39), 4.93 (0.61)	5%	0.012	0.219

λ_{em} : maximum emission wavelength; ϕ_F : fluorescence quantum yield determined using a calibrated integrating sphere; average lifetime: $\tau_{av} = (A_1\tau_1^2 + A_2\tau_2^2 + A_3\tau_3^2)/(A_1\tau_1 + A_2\tau_2 + A_3\tau_3)$; radiative transition rate constant: $k_r = \phi_F/\tau_{av}$; non-radiative transition rate constant: $k_{nr} = (1-\phi_F)/\tau_{av}$.

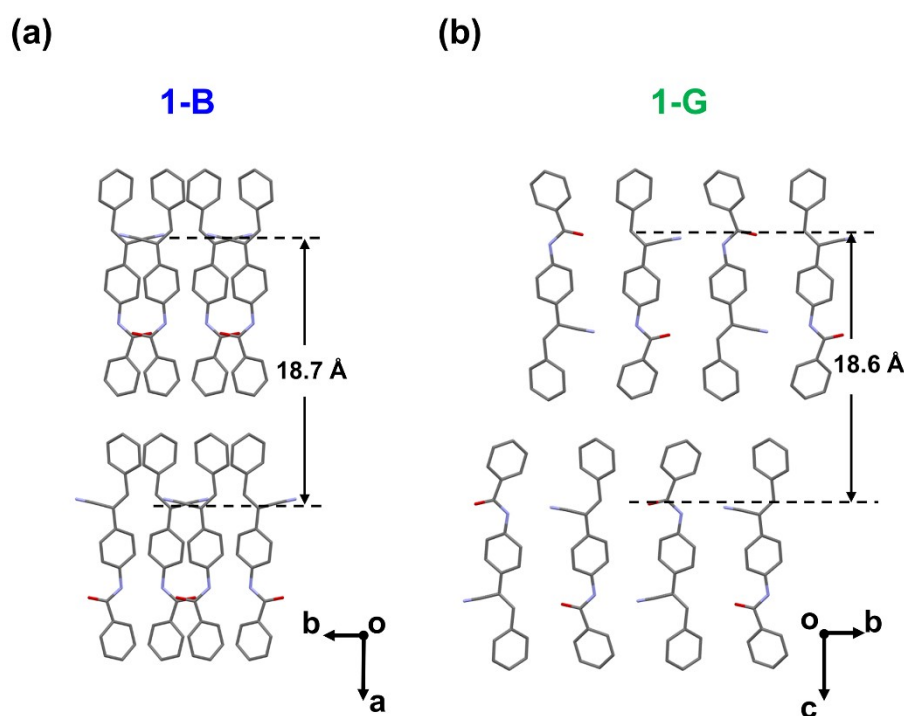
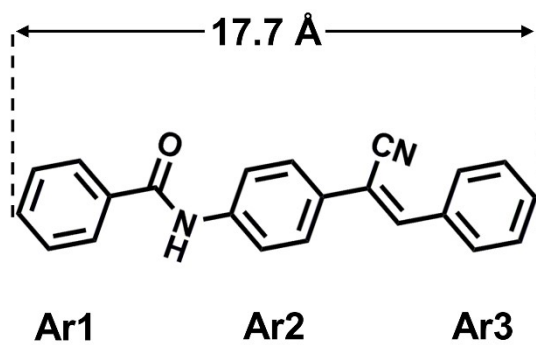


Fig. S5 Molecular layer packing structure of compound 1 in (a) 1-B and (b) 1-G.

Table S2. Details of crystallographic data for 1-B and 1-G.

	1-B	1-G
Empirical formula	C ₂₂ H ₁₆ N ₂ O	C ₂₂ H ₁₆ N ₂ O
Formula weight	324.37	324.37
Temperature	100(2) K	291 K
Wavelength	0.71073 Å	0.71073 Å
Crystal system, space group	Monoclinic, Cc	Monoclinic, P21/c
Unit cell dimensions	a = 36.442(3) Å α = 90° b = 6.0032(5) Å β = 97.296(3)° c = 7.3912(6) Å γ = 90°	a = 3.9543(2) Å α = 90° b = 11.5033(7) Å β = 92.144(2)° c = 35.785(2) Å γ = 90°
Volume	1603.8(2) Å ³	1626.61(16) Å ³
Z, Calculated density	4, 1.343 Mg m ⁻³	4, 1.325 Mg m ⁻³
Absorption coefficient	0.083 mm ⁻¹	0.082 mm ⁻¹
F(000)	680	680
Crystal size	0.11 x 0.09 x 0.08 mm	0.12 x 0.11 x 0.10 mm
2theta range for data collection	6.764-26.713°	5.772-53.568°
Limiting indices	-46<=h<=46, -7<=k<=7, -9<=l<=9	-5<=h<=4, -14<=k<=14, -45<=l<=45
Reflections collected/unique	14738/3395 [R(int) = 0.0415]	28375/3420 [R(int) = 0.0502]
Completeness to theta	99.8%	99.2%
Absorption correction	Semi-empirical from equivalents	Semi-empirical from equivalents
Max. and min. transmission	0.993 and 0.991	0.992 and 0.990
Refinement method	Full-matrix least-squares on F ²	Full-matrix least-squares on F ²
Data/restraints/parameters	3395/26/338	3420/0/226
Goodness-of-fit on F ²	0.986	1.170
Final R indices [I>2σ(I)]	R1 = 0.0425, wR2 = 0.1229	R1 = 0.0739, wR2 = 0.1598
R indices (all data)	R1 = 0.0561, wR2 = 0.1359	R1 = 0.0853, wR2 = 0.1654



	$\angle(\text{Ar1-Ar2})$	$\angle(\text{Ar2-Ar3})$
1-B	16.5°	51.9°
1-G	40.6°	43.2°

Fig. S6 Angle parameters and molecular length of compound 1 in 1-B and 1-G.

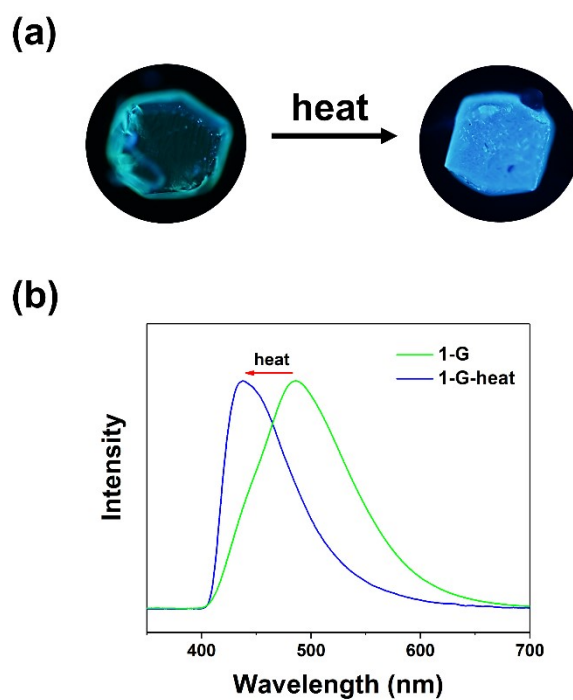


Fig. S7 (a) Fluorescent images and (b) fluorescence spectra of 1-G and heated sample.

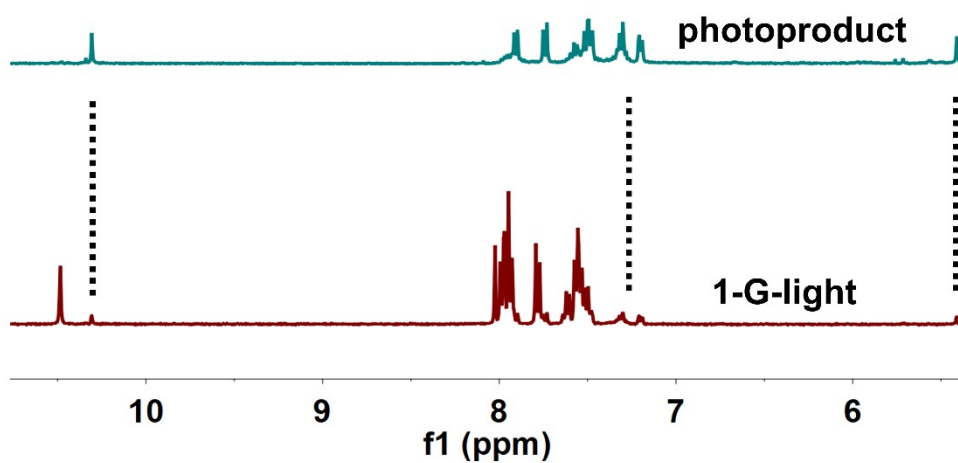


Fig. S8 ¹H NMR spectra of 1-G after irradiation and the purified photoproduct (cycloadduct).

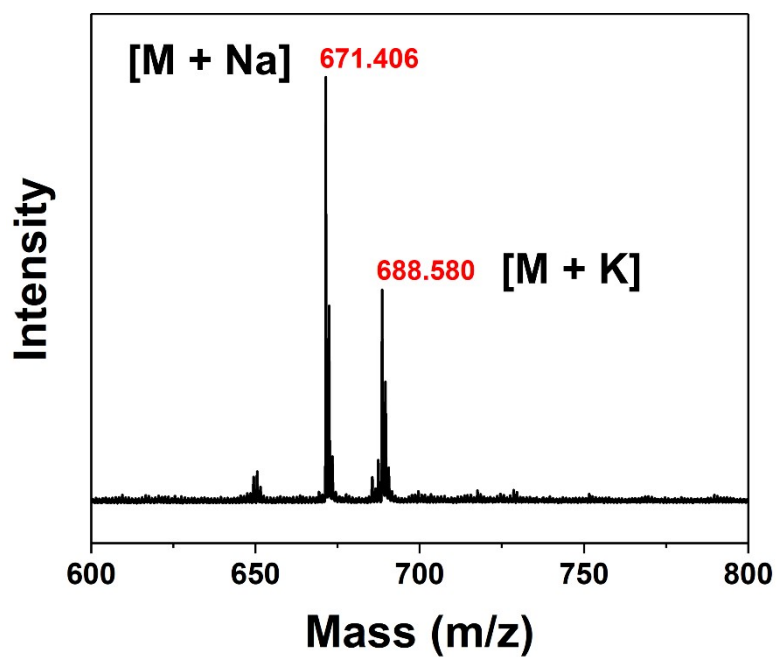


Fig. S9 MALDI-TOF result of the cycloadduct in DCM.

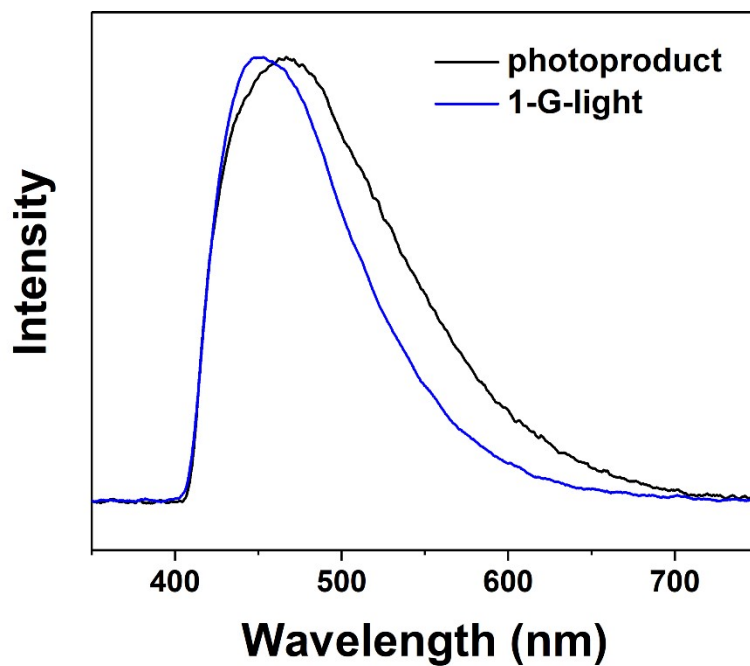


Fig. S10 Fluorescence spectra of 1-G after irradiation and the purified photoproduct (cycloadduct).

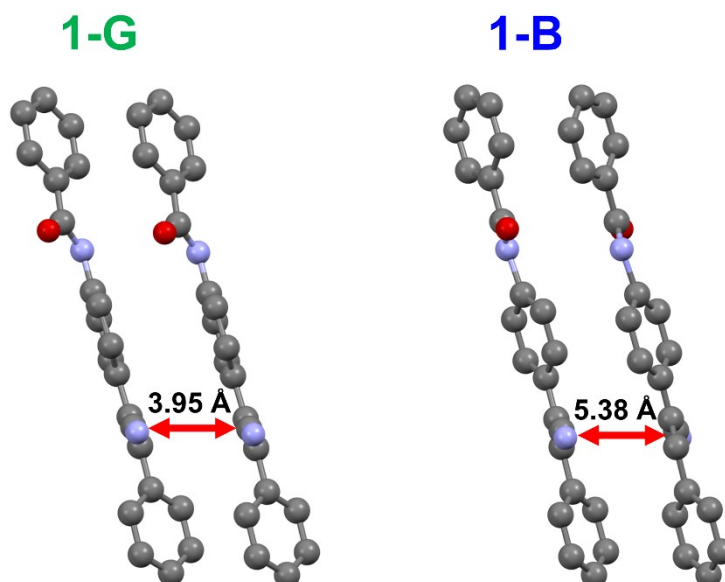


Fig. S11 The distances between the vinyl double bonds of neighbouring molecules in 1-G and 1-B.

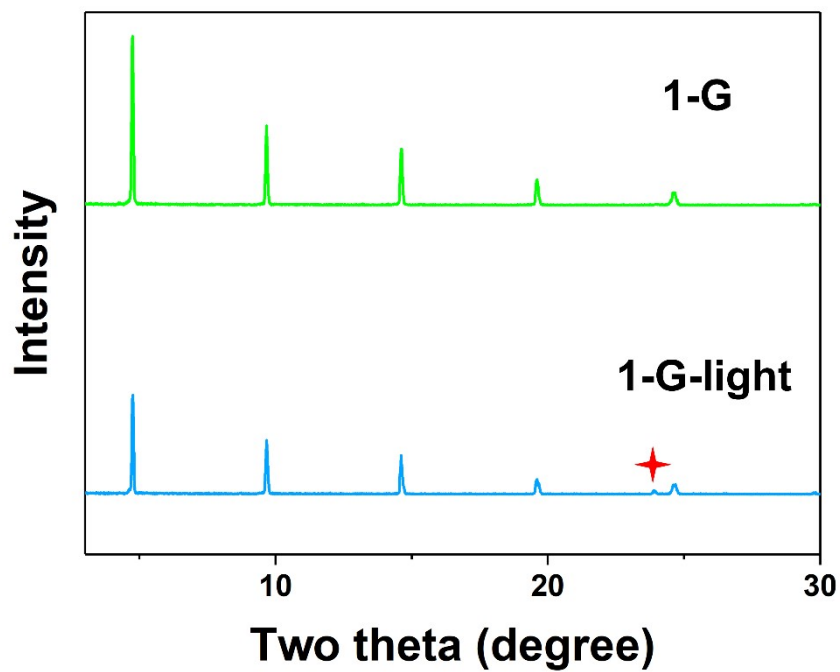


Fig. S12 XRD patterns of 1-G and 1-G-light.

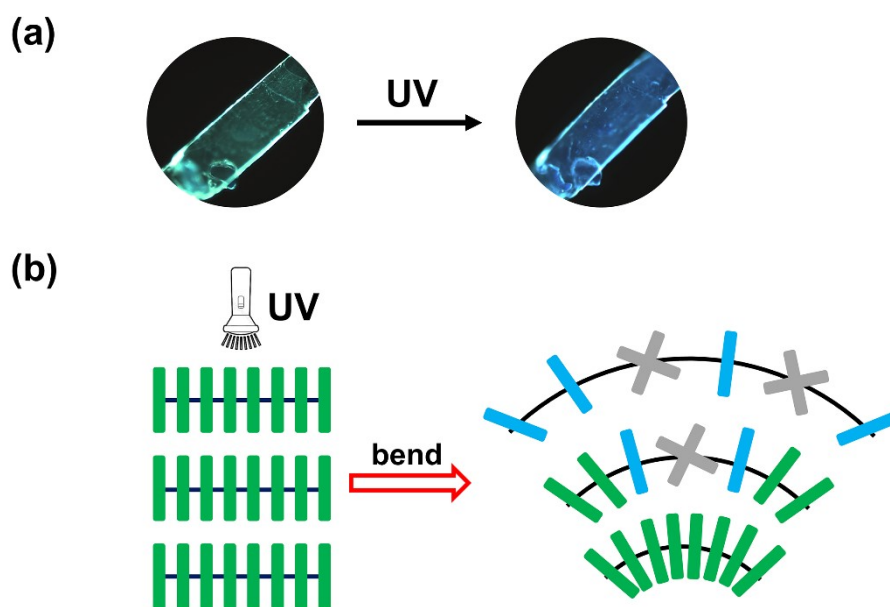


Fig. S13 Photoinduced bending of 1-G. (a) Fluorescent images of 1-G before and after UV irradiation. (b) Graphical presentation of the packing-structure variation under UV irradiation from the upper surface of 1-G.

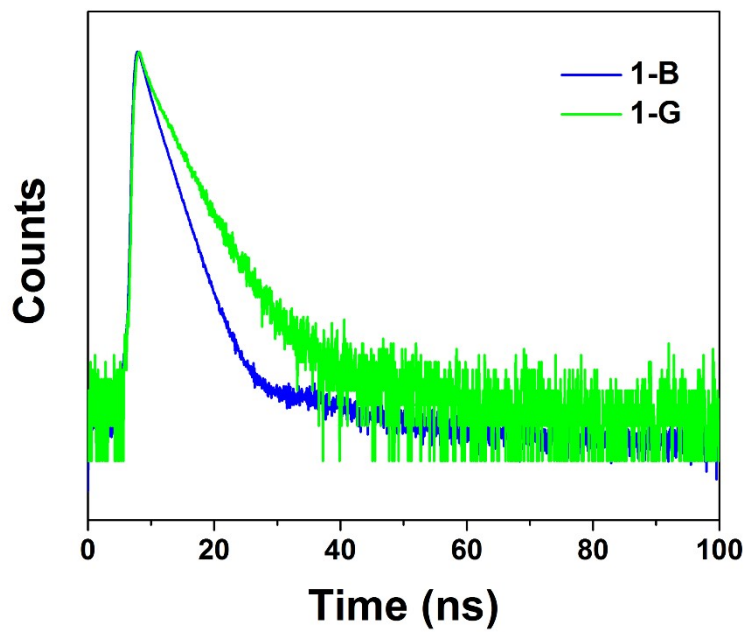


Fig. S14 Fluorescence decay profiles of 1-B and 1-G.

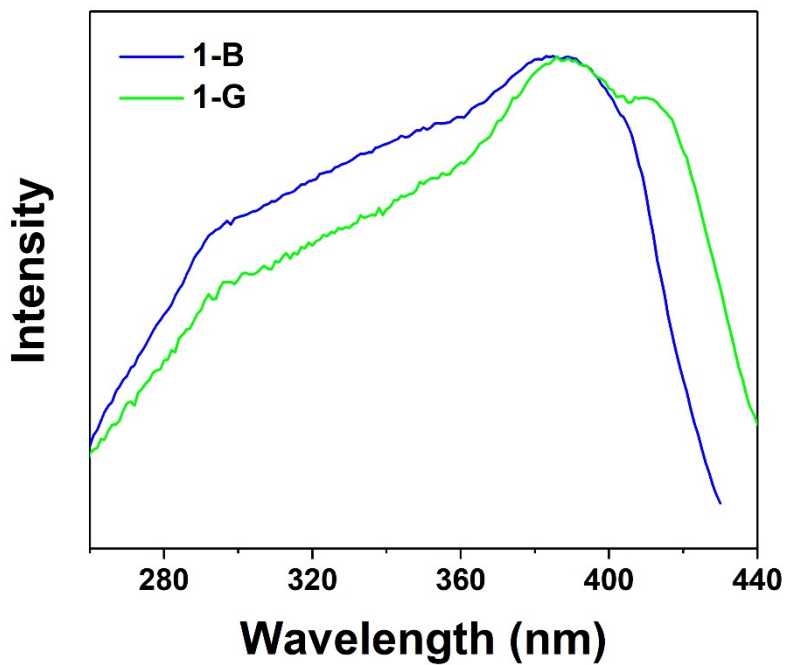


Fig. S15 Excitation spectra of 1-B and 1-G.

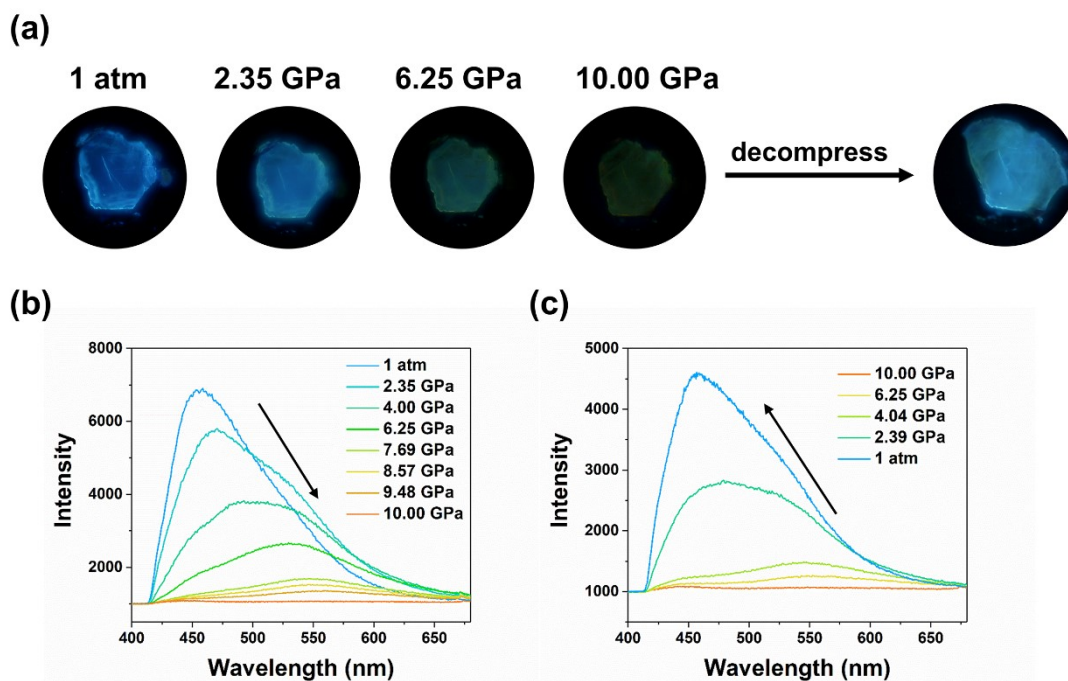


Fig. S16 (a) Fluorescent images of a single crystal of 1-G under reversible increasing and releasing hydrostatic pressures. (b) Fluorescence spectra of 1-G under reversible (b) increasing and (c) releasing hydrostatic pressures.

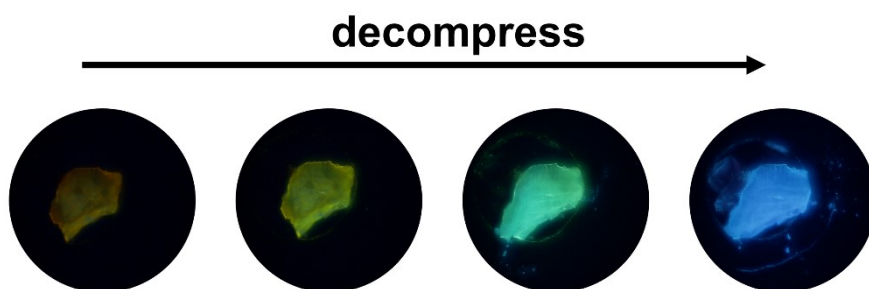


Fig. S17 Fluorescent images of 1-B under releasing pressures.

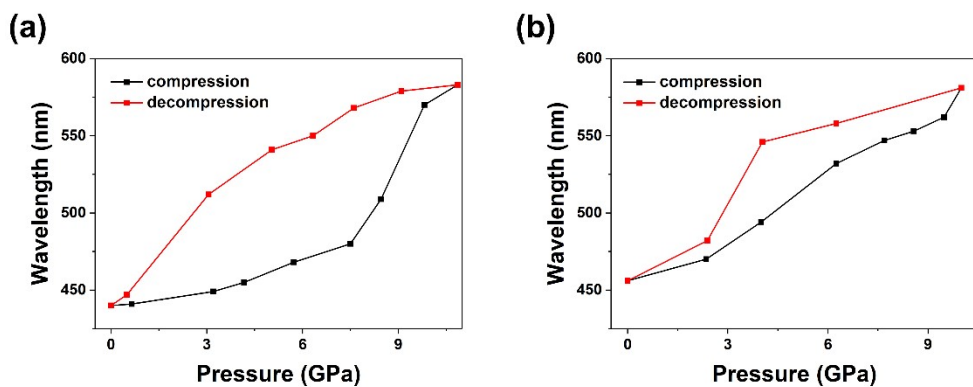


Fig. S18 Pressure versus the emission wavelength of (a) 1-B and (b) 1-G during increasing and releasing hydrostatic pressures.

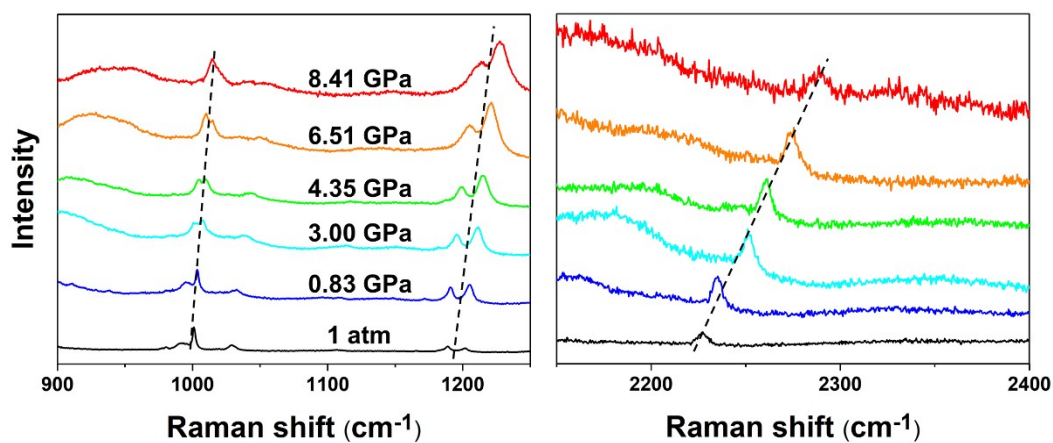


Fig. S19 Raman spectra of 1-B with under hydrostatic pressures. Excitation wavelength was 633 nm.